Speckle size, intensity and contrast measurement application in micron-size particle concentration assessment

Article *in* The European Physical Journal Applied Physics · December 2007

DOI: 10.1051/epjap:2007163

CITATIONS
26

READS
2,310

1 author:

Dan Chicea
Lucian Blaga University of Sibiu
95 PUBLICATIONS **277** CITATIONS

SEE PROFILE

Eur. Phys. J. Appl. Phys. **40**, 305–310 (2007)
DOI: 10.1051/epjap:2007163

THE EUROPEAN PHYSICAL JOURNAL
APPLIED PHYSICS

Speckle size, intensity and contrast measurement application in micron-size particle concentration assessment

D. Chicea[a]

Physics department, University Lucian Blaga, Str. Dr. Ion Ratiu 7–9, 550012 Sibiu, Romania

Received: 7 April 2007 / Accepted: 11 September 2007
Published online: 13 December 2007 –

Abstract. A transmission type of experiment was set-up to investigate coherent light scattering on suspensions with scattering centers having a wider size distribution. For each sample the contrast, the average intensity and the average speckle size of the far interference field were calculated using an alternative simple algorithm that is presented in detail. The variation of the far field parameters with the scattering centers concentration is presented. A possible application in measuring the scattering centers concentration in the very small values range is suggested and the range is indicated.

PACS. 42.30.Ms Speckle and moire patterns – 42.30.Va Image forming and processing

1 Introduction

When coherent light crosses a medium having scattering centers an un-uniformly illuminated image is obtained, currently named speckled image, having a statistical distribution of the intensity over the interference field. The speckled image appears as a result of the interference of the wavelets scattered by the scattering centers (SC hereafter), each wavelet having a different phase and amplitude in each location of the interference field. The image changes in time as a consequence of the scattering centers complex movement of sedimentation and Brownian motion giving the aspect of "boiling speckles" [1,2].

The speckled image can be observed either in free space and is named objective speckle or on the image plane of a diffuse object illuminated by a coherent source; it is named subjective speckle in [1]. The review paper [2] classifies the two types of speckled images as far field speckle and image speckle. In this work the objective speckle, respectively far field speckle is considered.

It was often pointed out in the literature that the speckle parameters like size, contrast, intensity and polarization carry information on the scattering media. Dynamical speckle analysis has become a current method to characterize the dynamic behavior of scattering medium such as flow, sediment and Brownian motion. The motion of the speckle field was analyzed by correlometric methods [3–5] or by laser speckle contrast analysis [6,7]. The speckle size can be used to measure the roughness of a surface [8–10] or to assess the thickness of semi-transparent thin slab like in [11]. Most of the above mentioned experiments use the backscattered speckle configuration. In papers like [12] a different optical set-up is used to measure the correlation function in the near field, and show the near-field speckle dependence on the particles size. The work reported in [13,14] uses a transmission optical set-up to measure the far field parameters like contrast and speckle size. The transmission type of setup was used in the work reported in this paper as well.

The work presented in this paper was performed to investigate the variation of the average statistical parameters of the far field that is the speckle size, intensity and contrast, with the SC concentration and to test an alternative, simpler, less computer time consuming algorithm for calculating the average speckle size. Most of the work reported in the literature presents results of light scattered by SCs having narrow size distribution, typically on latex micrometric balls. The SCs used in this work have a wider size distribution. Finally, the variation of the statistical parameters mentioned above with the SC concentration suggests that the method can be used in measuring the very small concentration of the SC and the range is indicated.

2 Experimental set-up and data processing procedure

The schematic of the experiment is presented in Figure 1. The He-Ne laser has a wavelength of 632.8 nm and a constant power of 2 mW. The coherence length is 20 cm, as stated by the producer (IFTAR). No polarizer was placed between the laser and the cuvette, but the light is linearly polarized, as the laser has Brewster windows. The active area of the glass cuvette was 12 mm thick. Measurements were done at 3.5 degrees from the beam axis

[a] e-mail: dan.chicea@ulbsibiu.ro

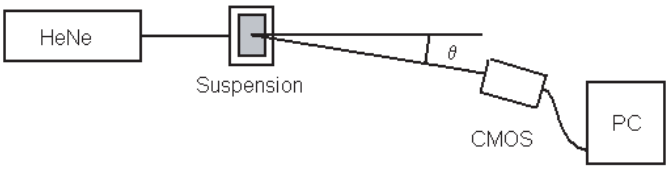

Fig. 1. The schematic of the experiment, view from above.

using a CMOS camera and data acquisition was done on a PC using the USB port. The laser – cuvette distance was 5 cm and the cuvette – CMOS camera distance was 55 cm. The optical system of the camera was removed; therefore the recorded images were the direct interference on the CMOS detection matrix. Consequently the far field speckle was recorded, not the speckle image.

The average contrast of the image, either acquired as a bitmap or extracted from the frames of the movie, is currently calculated [1,2] as:

$$C = \frac{\langle (I(i,j) - \langle I \rangle)^2 \rangle^{1/2}}{\langle I \rangle} \tag{1}$$

where $I(i,j) = I(xi, yj)$ is the intensity recorded by the cell (i,j) of the CMOS, hence by the pixel (i,j) of the array of pixels the image consists of. This is a space contrast and not a time contrast, as pointed out in [16]. In (1) the angular brackets stand for average over the entire 640×480 pixels collection of intensity values for an image that is processed. In the work described in this paper the image contrast is calculated with equation (1).

In [1,13–15] the average speckle size is calculated as the normalized autocovariance function of the intensity speckle pattern acquired in the observation plane:

$$c_l(\Delta x, \Delta y) = \frac{FT^{-1}\lfloor |FT[I(x,y)]|^2 \rfloor - \langle I(x,y) \rangle^2}{\langle I(x,y)^2 \rangle - \langle I(x,y) \rangle^2} \tag{2}$$

where FT is the Fourier transform, $\langle\rangle$ is a spatial average, $cl(\Delta x, 0)$ is a horizontal and $cl(0, \Delta y)$ a vertical profile. The $cl(\Delta y, \Delta y)$ function defined in (2) has a 0 base and the width of the function provides a reasonable measure of the speckle size, as stated in [15].

In this paper a different approach is proposed to calculate the speckle size. For each vertical profile of a frame the normalized autocorrelation function [17] was calculated as:

$$A_n(s) = \frac{\langle I(n,j) I(n, j+s) \rangle}{\langle I(n,j) I(n,j) \rangle} \tag{3}$$

where the angle brackets denote averages over the coordinate y, n represents the number of the vertical profile and s is the autocorrelation distance.

The speckle size for n-th profile, (the profile speckle size) is defined as the value of the s (pixel number or distance, if multiplied by the pixel size on the CMOS) where the autocorrelation function decreases to $1/e$. An average of the profile speckle sizes is calculated for each image and we define this average as the average speckle size for that particular image. A vertical profile is presented in Figure 2 and the autocorrelation function of that profile in

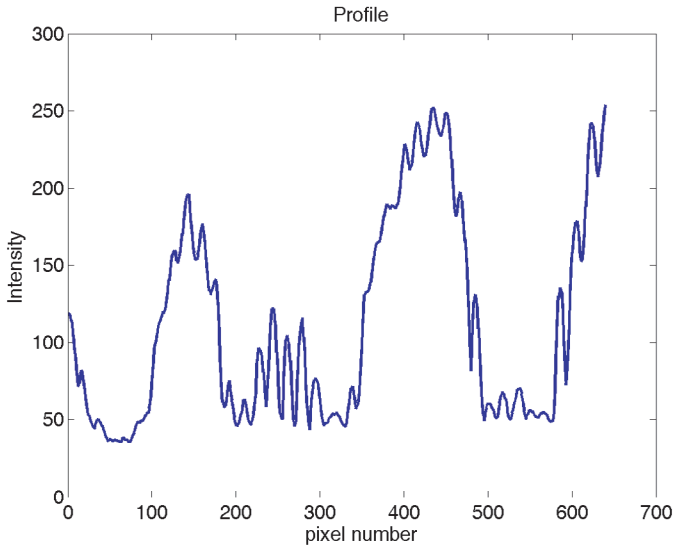

Fig. 2. A vertical intensity profile.

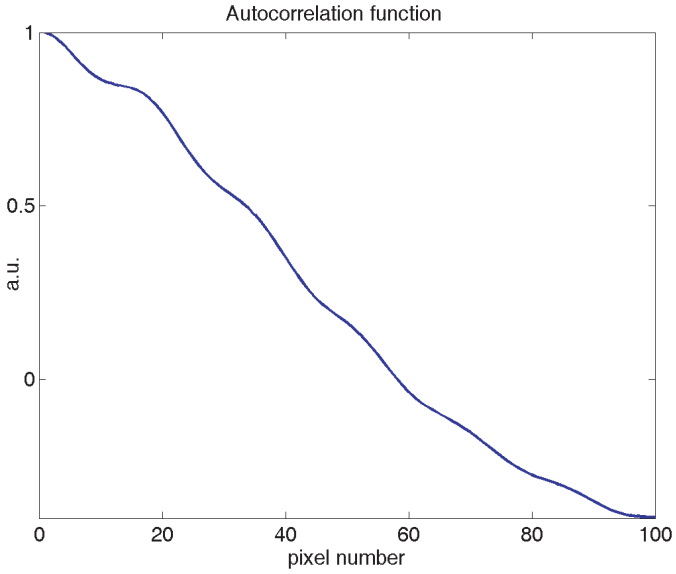

Fig. 3. The normalized autocorrelation function.

Figure 3. The profile speckle size for the profile in Figure 3 is 39 pixels.

The speckle size is expressed in pixels because this is the natural unit to calculate it in a digital image. On the CMOS conversion matrix we used, a pixel is a square having the side of 8.0 μm. In order to have the speckle size in meters, it must be multiplied with the pixel side size. When repeating the experiment with a different CMOS or using a different cuvette – CMOS distance a different speckle size will result, as described in [15].

The procedure that was used in this work is apart of the procedures described in [13–15] primarily because it is a lower cost procedure. In [13–15] a CCD with an analog to digital converter was used. In this work a simple CMOS camera was used, connected to a PC through an USB port. The acquisition was done on 24 bits rather than on 10 bits. The speckle correlation time measured in

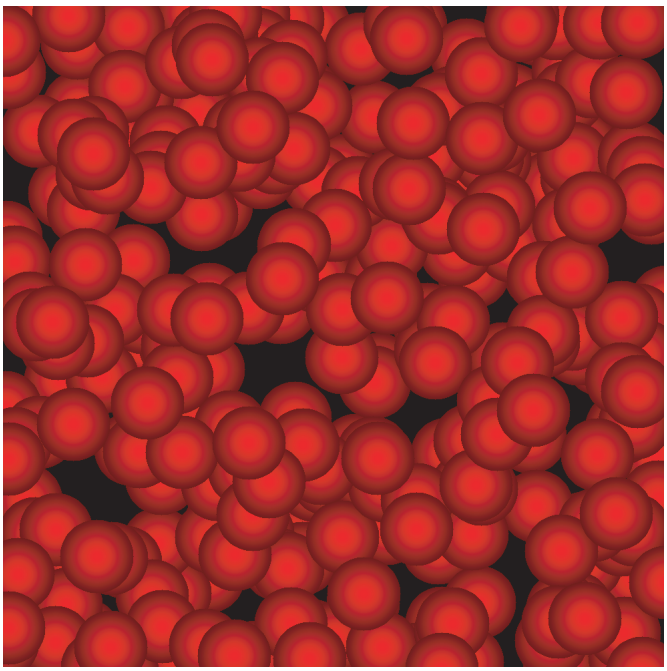

Fig. 4. A generated speckle image having the "speckles" randomly distributed over the area, each one have a size of 65 pixels.

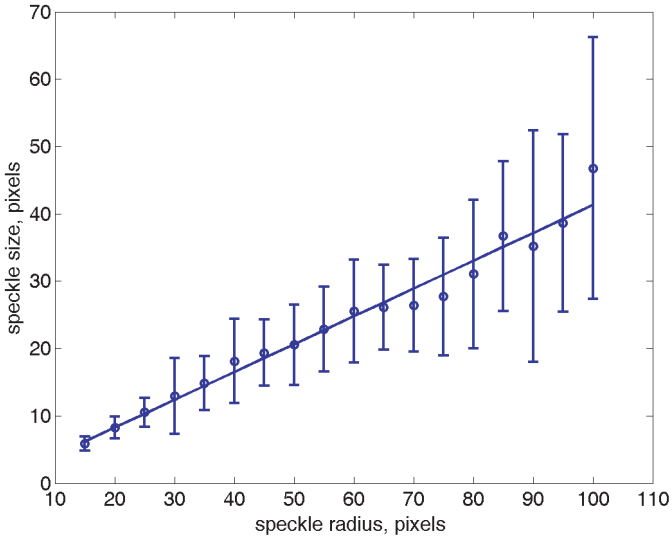

Fig. 5. The calculated speckle size, with error bars, versus the generated speckle radius. The linear regression equation is $y = 0.4130 \times x + 0.0101$.

a preliminary experiment was around 6 ms and the acquisition time was 1 ms. The images were acquired either as bitmaps or as uncompressed AVI. The program that was written to perform the calculations, as described above, first opens the conventional graphic formats and extracts the intensity array $I(x, y)$.

The algorithm was tested to verify if the algorithm described above for calculating the average speckle size produces a reasonable measure of the actual speckle size. For this purpose different type of speckle images were generated, having both a cosine and an exponentially decreasing profile from the center to the margin of each "speckle", with different simulated speckle sizes, placed either in rows or randomly over the calculated image, with speckles not overlapped and partially overlapped. The procedure was tested on the four types of generated images, as described above, each one being a 1000×1000, 24 bits color depth bitmap. Figure 4 presents a generated speckle image having the "speckles" randomly distributed over the area, each one have a size (diameter) of 65 pixels. We notice that the circular "speckles" are partially overlapped, which simulates well the real image, where the maxima are not equidistant. The speckle size and the error in assessing it were calculated for different radius values used in generating the images. The results are presented in Figure 5, where the circles are the calculated speckle sizes, with the estimated errors and the line represents the linear regression, described by equation (4):

$$Sps = 0.4130r + 0.0101. \tag{4}$$

In (4) Sps stands for the calculated speckle size and r for the radius of the generated "speckle". As the radius increased the error in calculating the speckle size increased, because the size of the bitmap remained constant, 1000×1000, but the number of generated speckles was consequently decreased, otherwise the degree of overlapping turned to be too big.

Examining the image presented in Figure 4, and the images of the other generated speckle images, not presented here, together with the plot in Figure 5, we can conclude that the procedure presented in this work, although it is less time consuming, provides not only a reasonable measure of the speckle size but the error in measuring it, as well. The error bars on the plots are the confidence intervals, l in (5) calculated using the Student test, considering 60 frames for each sample and a 99% confidence level, using:

$$l = tsn^{-\frac{1}{2}} \tag{5}$$

where t is the parameter of the Student test, s is the standard deviation and n is the number of data values in a set, that is the number of frames, 60 for this experiment.

Another difference of the speckle size calculation procedure presented here lays in the fact that consecutive images extracted form a recorded movie are processes and the results are averaged, rather than processing a single image, as [13–15]. Examining the plots of the average contrast (Fig. 7), speckle size and intensity (data not presented) derived from single bitmaps processing for each concentration (details are presented in Sect. 3) we notice a big spread of the data. This suggests that relatively big differences between pictures taken for the same sample at different moments might occur, due to fluctuations. The problem was solved in [13] by choosing a smaller cuvette – CCD distance, 36 cm, and in [15] 15 cm, in order to have a bigger number of speckles recorded. In the work described here, a different approach, described further on, was used.

In order to minimize the differences from one bitmap to another, in respect to the speckle size, the experiment was

repeated maintaining the cuvette – CMOS distance but recording more frames. An uncompressed, 24 bits color depth AVI type movie was recorded for each concentration, instead of a single bitmap, with the same resolution, 640×480 pixels, using a framerate of 1 per second. The speckle size was calculated for each frame using the algorithm described above and an average was calculated for the set of individual values, giving the speckle size for that particular sample. A previous experiment using a data acquisition system revealed that the autocorrelation time for this type of samples is around 0.1 seconds therefore a framerate of 1 per second assures that the images in consecutive frames are not correlated and that the average over the 60 frames for each sample does not depend on the specific time they were recorded at.

Finally, the algorithm that is proposed in this paper is less computer time consuming as it does not require the calculation of the Fourier transform on the 640×480 array twice (the elapsed calculation time goes as $(640 \times 6460)^2$), but the autocorrelation function for 480 vectors of 640 elements each (the elapsed calculation time goes as 480×640^2). In addition the procedure provides, together with the average speckle size, the error in speckle size calculation, as described above, in (5). It should be noted thought that the computation time difference is negligible if one single bitmap is processed, but becomes significant when processing big resolution bitmaps (more than 10^6 pixels), movies, or sets of movies, in batch mode, as described further on. Moreover, as technology develops, faster and higher resolution CCDs will become commercially available and the gain in computation time might become appealing in developing an online, automatic procedure for monitoring low SC concentration, as suggested at the end of Section 4.

3 Results

First a preliminary experiment was conducted, by recording the far field speckle produced by light scattering on whole milk suspension in deionized water at different dilutions. The unprocessed milk has a wide distribution of the particles ranging between 1 and 10 μm for the milk fat particles with a maximum on 4 μm [18]. In [19] it is stated that two modes can be detected in each sample, one relating to the fat phase and one relating to free casein micelles. In moving from full fat to skimmed milk the relative proportions in each mode changes, tracking the reduction in fat content. Full fat milk was used in this paper therefore the SC had a wide size distribution, ranging from 0.05 μm from casein micelles to 10 μm for milk fat particles, as presented in the plots [18,19].

In the first part of the experiment a 24 bits color depth bitmap image, having a resolution of 640×480 pixels was recorded for different milk concentrations. Figure 6 presents the bitmap recorded for diluted milk samples having the volume ratios (calculated as whole milk volume divided by the diluted suspension volume) of 0.0372.

Using a program written for this purpose with the algorithm described in Section 3 the average intensity over the recorded area, the average contrast and the average speckle size, in pixels, were calculated. First one frame was acquired for each sample (concentration). The variation of the average contrast with the concentration, expressed as volume ratio, for whole milk diluted in deionized water is presented in Figure 7.

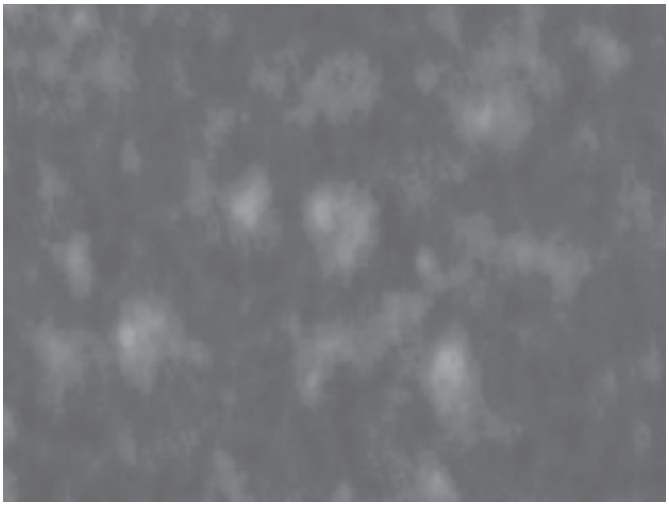

Fig. 6. The far field speckle for diluted whole milk having the volume ratio of 0.0372.

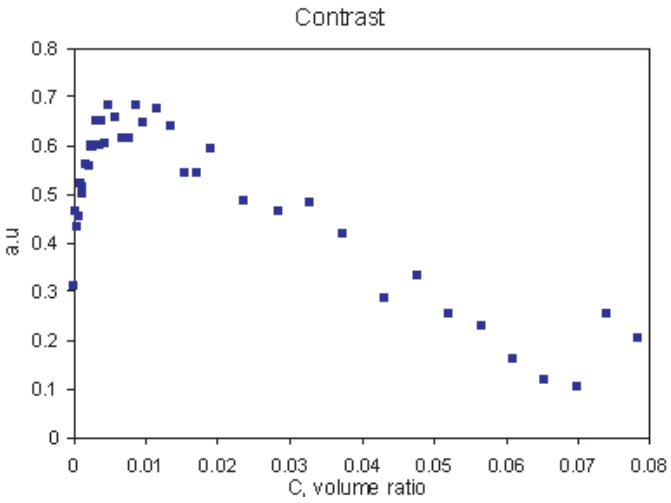

Fig. 7. The average contrast variation with the concentration.

As previously mentioned, the data has a big spread. The spread was minimized by recording a set of 60 consecutive frames for each sample and averages of the intensity, contrast and speckle size were calculated. Figure 8 presents the variation of the average intensity, Figure 9 the variation of the contrast and Figure 10 the variation of the average speckle size with the concentration.

4 Discussions

Examining Figure 8 we notice that at very small SC concentration the average intensity increases with the

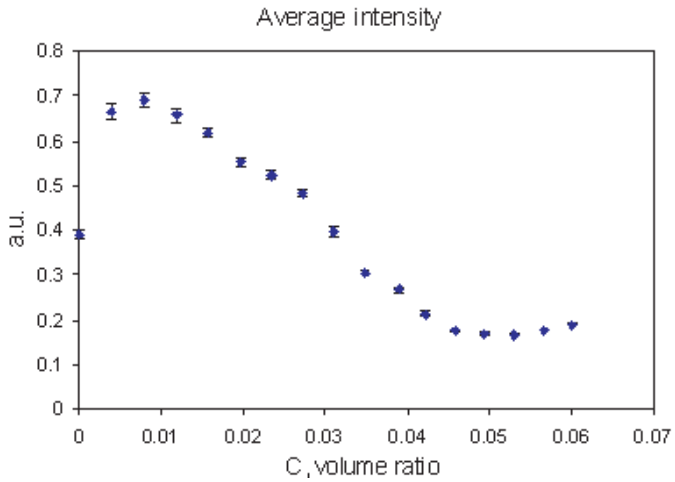

Fig. 8. The average intensity variation with the concentration.

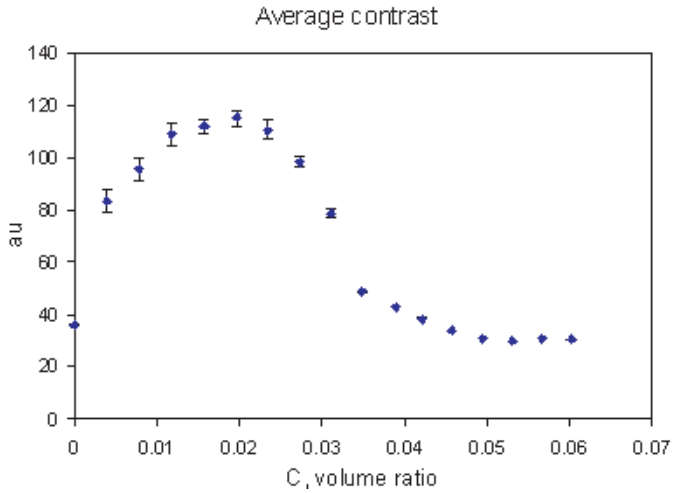

Fig. 9. The average contrast variation with the concentration.

concentration, presents a maximum and then decreases with the concentration, in the range where multiple scattering is dominant. In the big concentration range the average intensity remains constant. This result is similar with the work reported in [20], where light SCs were red blood cells.

The average contrast has a very fast increase with the SC concentration increase, displays a plateau and a fast decrease, as revealed by Figure 9. As the concentration increases the absolute value of the slope decreases and finally the contrast remains constant. This result is similar with the results reported in [13] on latex microspheres, not on diluted milk, although at a first look the plot in Figure 9 displays a plateau while [13] presents an almost linear decrease. Moreover, in [13] the decrease for 0.2 μm diameter microspheres is similar with the contrast decrease reported in this work, except for the plateau in the big concentration range. This can be explained by the much bigger concentration range used in this work, in the range [0.0039–0.060] (volume ratio), where the optical depth estimation leads to values bigger than 100 for the right margin of the interval, deep in the multiple scattering range.

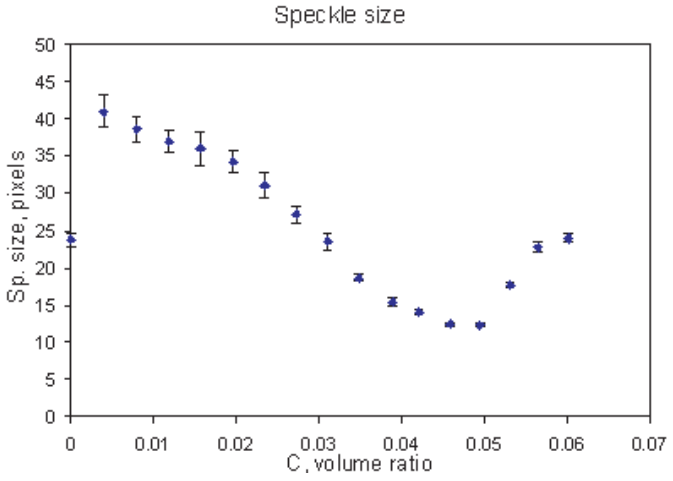

Fig. 10. The average speckle size variation with the concentration.

The concentration range reported in [13] is much narrower as the optical depth range is approximately [0.2–2.2]. If a small area in the plot in Figure 8 corresponding to this narrow range is taken, the plot appears linear.

The other parameter that was calculated in this work is the average speckle size. The average speckle size presents a constant decrease with the SC concentration and a slight increase in the big concentration range, as presented in Figure 10. The linear decrease is similar with the results reported in [13]. The increase presented in Figure 10 is different of the results reported [13] and the difference can be explained by the concentration range used in this work, which covers a wider range than in [13], deeper in the multiple scattering range, as described above. Again, if a small range is extracted from the plot in Figure 10, a linear variation will appear. Furthermore, the work in [13] presents results on skimmed and on semi-skimmed milk, while in the work reported in this paper whole milk was used, which has a wider size particle distribution.

Examining the plot of the average intensity variation with the concentration (Fig. 8) expressed as volume ratio we notice that the curve can be used a calibration curve for measuring the concentration in the [0.01–0.045] volume ratio range. Moreover, the average speckle size (Fig. 10) has a monotone variation with the concentration over a wider concentration range, that is [0.004–0.045] and this variation can be used in developing an online, automatic procedure for monitoring low SC concentration. For this purpose, calibration curves have to be drawn first, by measuring the average intensity and speckle size for samples with a precisely adjusted concentration, in the [0.004–0.045] volume ratio range. The curves can be used later on to measure the concentration for an unknown diluted milk sample. As themselves, any of these suggested procedures must be used together with a different procedure that establishes without doubt that the concentration is not outside the indicated range.

Figure 9 reveals that the contrast variation with the volume ratio does not display almost linear variation as do the average intensity (Fig. 8) and the average speckle

size (Fig. 9) on a relatively extended concentration range; therefore the contrast variation appears less suited to be used in a concentration measurement procedure.

5 Conclusion

The similarity of the results presented in this paper with the results reported in the literature on similar type of samples reveal that the average speckle calculation algorithm presented in this paper provides a reasonable measure of the speckle size. They also reveal that the average intensity together with the average speckle size of the far field can be used as a fast procedure in assessing the scattering centers concentration in a biological fluid, in a small and limited concentration range though, if they are used together with a different procedure that establishes without doubt that the concentration is not outside the indicated range.

References

1. J.W. Goodman, Statistical Properties of Laser Speckle Patterns, in *Laser speckle and related phenomena*, edited by J.C. Dainty (Springer-Verlag, Berlin, Heidelberg, New York, Tokyo, 1984), Vol. 9
2. J.D. Briers, Physiol. Meas. **22**, R35 (2001)
3. D.A. Boas, A.G. Yodh, J. Opt. Soc. Am. A **14**, 192 (1997)
4. Y. Aizu, T. Asakura, Opt. Laser Technol. **23**, 205 (1991)
5. I.V. Fedosov, V.V. Tuchin, Proc. SPIE **4434**, 192 (2001)
6. J.D. Briers, G. Richards, X.W. He, J. Biomed. Opt. **4**, 164 (1999)
7. D.A. Zimnyakov, J.D. Briers, V.V. Tuchin, in *Handbook of biomedical diagnostics*, edited by V.V. Tuchin (SPIE Press, Bellingham, 2002), Chap. 18
8. P. Lehmann, Appl. Opt. **38**, 1144 (1999)
9. G. DaCosta, J. Ferrari, Appl. Opt. **36**, 5231 (1997)
10. R. Berlasso, F.P. Quintian, M.A. Rebollo, C.A. Raffo, N.G. Gaggioli, Appl. Opt. **39**, 5811 (2000)
11. A. Sadhwani, K.T. Schomaker, G.J. Tearney, N.S. Nishioka, Appl. Opt. **35**, 5727 (1996)
12. M. Giglio, M. Carpineti, A. Vailati, D. Brogioli, Appl. Opt. **40**, 4036 (2001)
13. Y. Piederrière, J. Cariou, Y. Guern, B. Le Jeune, G. Le Brun, J. Lotrian, Opt. Express **12**, 176, (2004)
14. Y. Piederriere, J. Le Meur, J. Cariou, J.F. Abgrall, M.T. Blouch, Opt. Express **12**, 4596, (2004)
15. Y. Piederriere, F. Boulvert, J. Cariou, B. Le Jeune, Y. Guern, G. Le Brun, Opt. Express **13**, 5030 (2005)
16. R. Nothdurft, G. Yao, Opt. Express **13**, 10034 (2005)
17. R. Bracewell, *The Fourier Transform and Its Applications*, 3rd edn. (McGraw-Hill, New York, 1999)
18. M.C. Michalski, F. Michel, C. Geneste, Lait **82**, 193 (2002) `http://www.edpsciences.org/articles/lait/pdf/2002/02/04.pdf?access=ok`
19. Laser Diffraction Particle Size Measurement of Food and Dairy Emulsions – Supplier Data by Malvern, `http://www.azom.com/details.asp?ArticleID=2808`
20. I. Turcu, Appl. Opt. **45**, 639 (2005)